

Supporting Information:

Penetration of nanoparticles across a lipid bilayer: Effects of particle stiffness and surface hydrophobicity

Shuo Wang^a, Hui Guo^b, Yinfeng Li^{*,a} and Xuejin Li^{*,c}

^aDepartment of Engineering Mechanics, School of Naval Architecture, Ocean and Civil Engineering (State Key Laboratory of Ocean Engineering, MOE Key Laboratory of Hydrodynamics), Shanghai Jiao Tong University, Shanghai 200240, P. R. China

^bDepartment of Urology, Shanghai Jiao Tong University Affiliated Sixth People's Hospital, Shanghai 200233, P. R. China

^cDepartment of Engineering Mechanics and Key Laboratory of Soft Machines and Smart Devices of Zhejiang Province, Zhejiang University, Hangzhou 310027, P. R. China

The deformation analysis of the NPs during the penetration process

To support our assumption quantitatively, we investigate the deformation of NPs with different stiffness and hydrophilicity. Fig. S1a plots the maximal distance of beads on the hydrophilic NPs in the transverse plane, and the abscissa axis is the time steps of the simulation. We find that the hydrophilic NPs deforms to a flat spherical during penetration, the size of NPs with softer stiffness are greater, which means that the NPs are flatter. Fig. S1b shows the length change of hydrophobic NPs in Z direction, in which we find that the greater softness leads to more severe deformation of NPs along Z direction. Thus, we conclude that different stiffness indeed affects the deformation during the penetration process, resulting in different penetrating abilities.

* Corresponding author. E-mail address: liyinfeng@sjtu.edu.cn (Y. Li); xuejin_li@zju.edu.cn (X. Li)

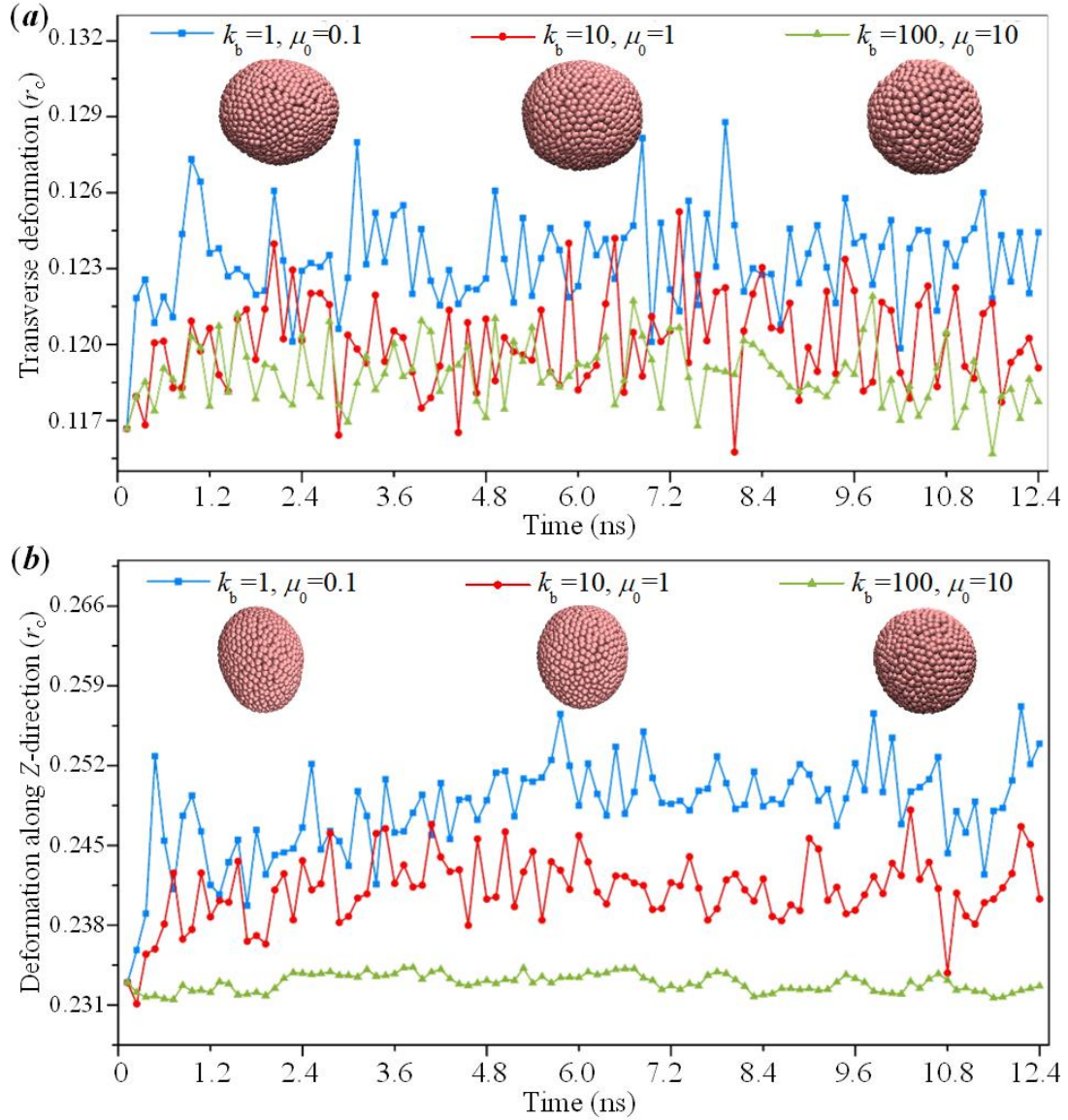


Fig. S1 Deformation of (a) hydrophilic and (b) hydrophobic NPs with different stiffness and hydrophobicity during the penetration process across a cell membrane.

A. The boundary condition of the membrane

To minimize the impact of the boundary conditions to the membrane relaxing, only the lipid heads of one edge of the lower lipid layer (blue beads in Fig. S2) are frozen so that the displacement of membrane in Z direction is fixed. After relaxing for 12.16 ns, the constrained beads will move in X and Y directions and spread among the membrane (Fig. S2c).

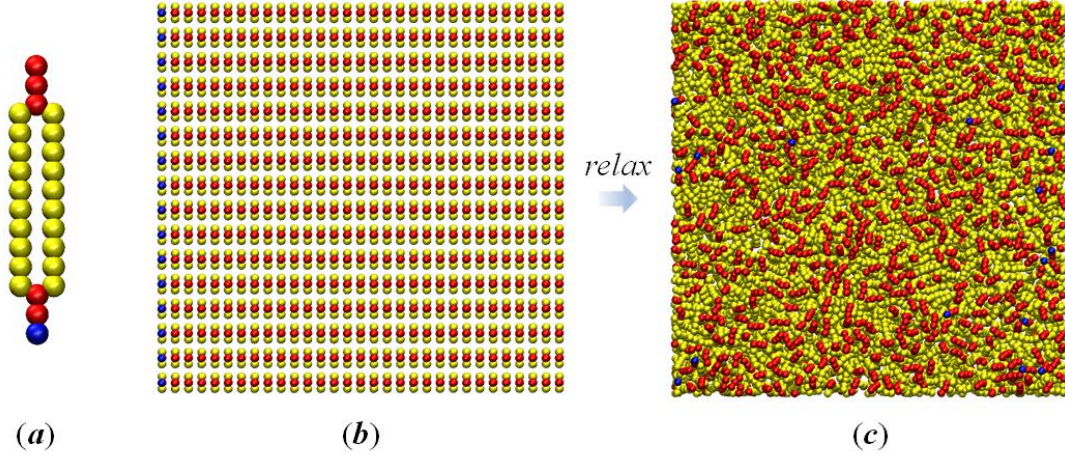


Fig. S2 Boundary conditions of the membrane.

B. Stiffness of the NPs

In our simulation, k_b and μ_0 determine the stiffness cohesively, and these two parameters have different effect on the NPs. k_b represents the bending constant of dihedral angles mainly influencing the local stiffness, while μ_0 mainly influence the global stiffness by applying a small engineering shear strain γ to the hexagonal network (Fig. S3). An increase in one (or both) of these two parameters can result in the increase of stiffness.

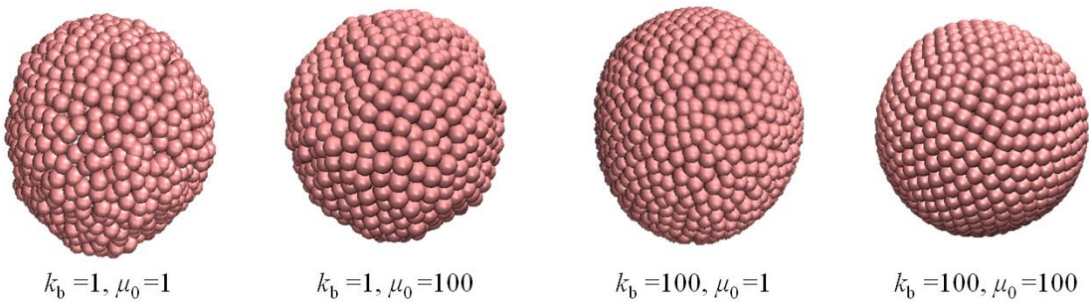


Fig. S3 Different deformation modes of different k_b and μ_0 .

To further evaluate the stiffness of soft NPs with different k_b and μ_0 , the stretching response experiments are performed. A pair of increasing forces are applied at the opposite edges of the NPs and the stretching distances are monitored (Fig. S4). The

approximated Young's modulus of NPs are estimated to be $E = 4.52$ MPa ($k_b = 0.1$ and $\mu_0 = 1.0$), 8.97 MPa ($k_b = 1.0$ and $\mu_0 = 10.0$), and 57.62 MPa ($k_b = 10.0$ and $\mu_0 = 100.0$). As a comparison, the Young's modulus of hydrogels varies from 0.1 MPa to 10.0 MPa.

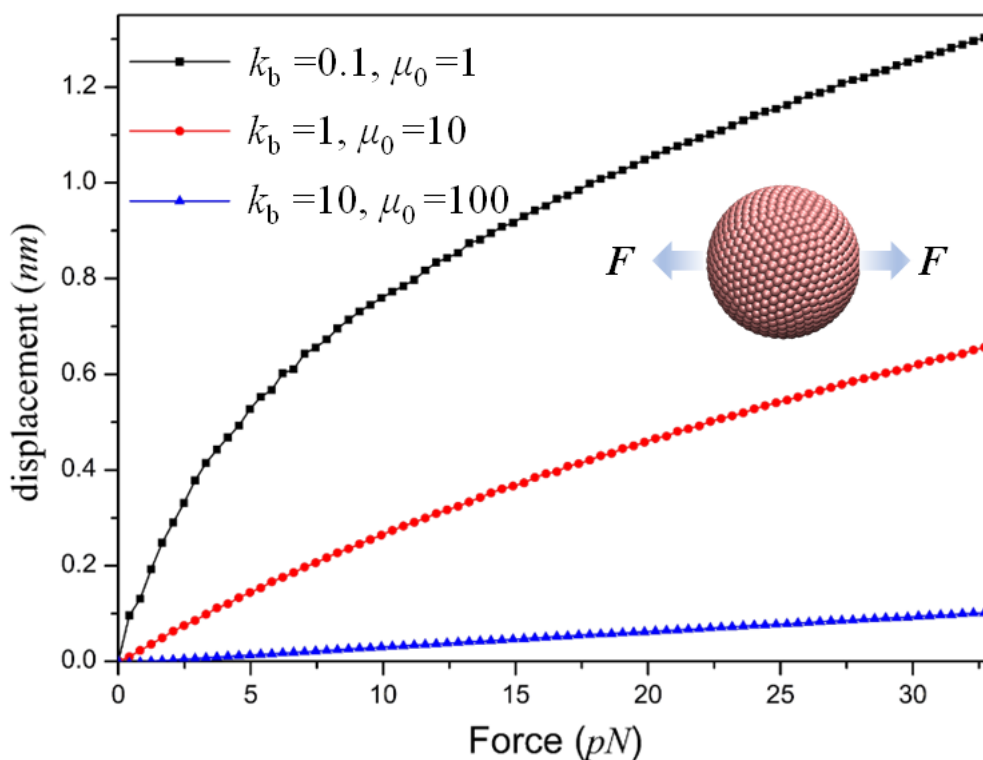


Fig. S4 Stretching response simulation of soft NPs with different k_b and μ_0 .

C. Methods of free energy calculations

To understand the effect of the stiffness of NPs during the penetration process, we calculate the change in free energy as a function of the distance between the particle center and the bilayer midplane by the way of constrained thermodynamic integration (TI).

To determine the free energy change of a NP as it penetrates through the membrane, we adopt a parameter λ to measure the normalized distance from the NP center to the midplane of membrane as

$$z(\lambda) = z(\lambda = 0) + \lambda [z(\lambda = 1) - z(\lambda = 0)] \quad (1)$$

Here, λ is set to 0 when the NP stands at an initial position above the lipid bilayer. As the NP penetrates through the membrane, λ gradually increases and finally reaches 1 when the NP arrives at the membrane midplane. The free energy change in this process is expressed as:

$$\Delta F = \int_0^1 \frac{\partial F(\lambda)}{\partial \lambda} d\lambda \quad (2)$$

According to eqn (2), we discretize the NP penetration path by choosing a series of λ values between 0 and 1. For each chosen value of λ , a harmonic potential

$$U(\lambda) = \frac{k_z}{2} [Z - z(\lambda)]^2 \quad (3)$$

is imposed to confine the motion of the NP in the z -direction, where $k_z = 1000$ and $z(\lambda)$ are the spring constant and equilibrium position of the potential, respectively; Z is the position of the NP center. Under the harmonic constraint, the NP is forced to oscillate around a pseudo-equilibrium position $\langle Z \rangle$ in the vicinity of $z(\lambda)$, where $\langle Z \rangle$ is the ensemble-averaged position of the NP center. The derivative of the free energy is determined from the constrained interaction between the NP and its surrounding as

$$\frac{\partial F(\lambda)}{\partial \lambda} = \left\langle \frac{\partial U(\lambda)}{\partial \lambda} \right\rangle \quad (4)$$

The integrand of eqn (4) is thus obtained from the simulated value of $\langle Z \rangle$ as:

$$\frac{\partial F(\lambda)}{\partial \lambda} = k_z [\langle Z \rangle - z(\lambda)] \quad z(\lambda = 0) \quad (5)$$

Integrating this expression allows the free energy change to be determined as a function of distance from the bilayer midplane,

$$\Delta F = \int_{z(\lambda=0)}^{z(\lambda=\varepsilon)} k_z [z(\lambda) - \langle Z \rangle] dz, \quad (0 \leq \varepsilon \leq 1) \quad (6)$$

Based on equation (6), we calculated the free energy change of the penetration process for NPs as a function of the distance between the particle center and the membrane midplane, as displayed in Fig. 4 in the main text.

D. Equivalent contact areas in the whole process

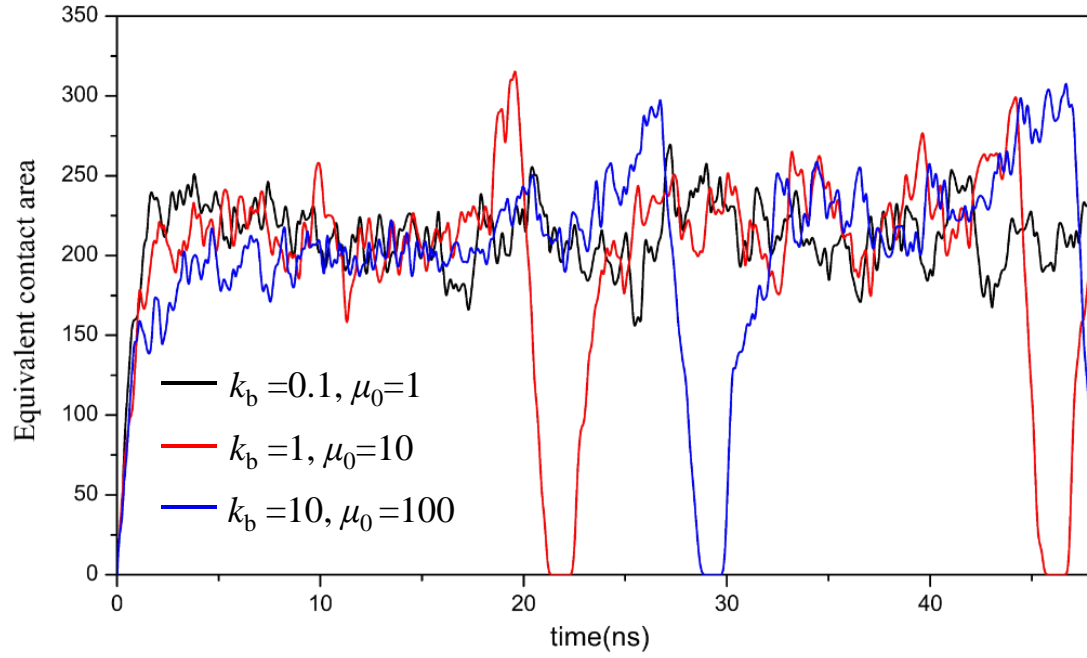


Fig. S5 Equivalent contact areas in the whole process